

Identifying predictable foraging habitats for a wide-ranging marine predator using ensemble ecological niche models

Kylie L. Scales^{*1,2,3}, Peter I. Miller¹, Simon N. Ingram⁴, Elliott L. Hazen³, Steven J. Bograd³,
Richard A. Phillips⁵

1. Plymouth Marine Laboratory, Prospect Place, Plymouth PL1 3DH, UK
2. Institute of Marine Sciences, University of California Santa Cruz, CA 95064, USA
3. National Oceanic and Atmospheric Administration (NOAA) Southwest Fisheries Science Center, Environmental Research Division, 99 Pacific Street, Suite 255A, Monterey CA 93940, USA
4. Marine Biology and Ecology Research Centre, Plymouth University, Plymouth PL4 8AA, UK
5. British Antarctic Survey, Natural Environment Research Council, High Cross, Madingley Road, Cambridge CB3 0ET, UK

Running title: *Modelling habitat suitability for a marine predator*

ABSTRACT

Aim

Ecological niche modelling can provide valuable insight into species' environmental preferences, and aid in identification of key habitats for populations of conservation concern. Here, we integrate biologging, satellite remote-sensing and ensemble ecological niche models (EENM) to identify predictable foraging habitats for a globally important population of the grey-headed albatross (GHA) *Thalassarche chrysostoma*.

Location

Bird Island, South Georgia; Southern Atlantic Ocean

Methods

GPS and geolocation-immersion loggers were used to track at-sea movements and activity patterns of GHA over two breeding seasons (n=55; brood-guard). Immersion frequency (landings per 10-minute interval) was used to define foraging events. EENM combining Generalised Additive Models (GAM), MaxEnt, Random Forest (RF) and Boosted Regression Trees (BRT) identified the biophysical conditions characterising the locations of foraging events, using time-matched oceanographic predictors (Sea Surface Temperature, SST;

chlorophyll-*a*, chl-*a*; thermal front frequency, *TFreq*; depth). Model performance was assessed through iterative cross-validation, and extrapolative performance through cross-validation between years.

Results

Predictable foraging habitats identified by EENM spanned neritic (<500m), shelf-break and oceanic waters, coinciding with a set of persistent biophysical conditions characterised by particular thermal ranges (3-8°C, 12-13°C), elevated primary productivity (chl-*a* > 0.5mg m⁻³) and frequent manifestation of mesoscale thermal fronts (*TFreq* > 25%). Our results confirmed previous suggestions that GHA utilise oceanic fronts, and objectively identified the Antarctic Polar Frontal Zone (APFZ) as suitable foraging habitat.

Over the spatial and temporal scales investigated here, performance of EENM was superior to that of single-algorithm models. In particular, MaxEnt performed poorly, resulting in highly variable predictions and exclusion from final EENM. Resultant EENM displayed good extrapolative performance between years.

Main Conclusions

EENM techniques are useful for integrating the predictions of several single-algorithm models, reducing potential bias. Our analysis highlights the value of EENM for use with movement data in identifying at-sea habitats of wide-ranging marine predators, with clear implications for conservation and management.

Keywords:

albatross; biologging; Boosted Regression Trees; front map; GAM; habitat model; ocean front; Random Forest; satellite remote sensing

1 (A) Introduction

2
3 Ecological niche modelling (also referred to as *species-habitat*, *predictive habitat*, *habitat-*
4 *based* and *species distribution modelling*) provides a framework for understanding species'
5 distributions as a function of their environmental preferences, and for identifying priority
6 areas for conservation. Understanding the mechanisms that underlie environmental preference
7 is particularly challenging for highly mobile species with complex life histories, especially in
8 the marine realm where conditions are dynamic. Recent efforts to integrate animal tracking
9 ('biologging'), satellite remote-sensing and ecological niche modelling have generated
10 valuable insights into the interactions between highly mobile marine species and the oceanic
11 environment (e.g. Torres *et al.*, 2015; Howell *et al.*, 2015; Raymond *et al.*, 2015). However,
12 most studies utilise a single modelling framework with its specific biases, reducing the
13 comparability of results and potentially limiting predictive capacity. An alternative is to
14 adopt an ensemble ecological niche modelling approach (EENM; Araújo & New 2007),
15 which combines the output of multiple model algorithms into one predictive surface and has
16 been used successfully for identifying key habitats for marine predators, including sea turtles
17 (Pikesley *et al.*, 2013) and seabirds (Oppel *et al.*, 2012).

18
19 Predicting the locations of suitable foraging habitats for wide-ranging pelagic species such as
20 procellariiform seabirds (albatrosses, petrels and shearwaters) is non-trivial, given the
21 complex and scale-dependent interactions between oceanographic processes and prey field
22 dynamics, and the diverse aspects of bird physiology, energetics, reproductive and other
23 constraints that govern foraging behaviour. The spatial ecology of pelagic seabirds appears to
24 be influenced by processes both extrinsic and intrinsic to each individual. For example,
25 habitat preferences of Southern Ocean seabirds vary among species (Commins *et al.*, 2014),
26 populations (Nel *et al.*, 2001, Louzao *et al.*, 2011, Joiris & Dochy 2013), and individuals
27 (Phillips *et al.*, 2006; Patrick & Weimerskirch 2014); between sexes (Phillips *et al.*, 2004);
28 between life history stages (Phillips *et al.*, 2005); through the annual cycle (Phillips *et al.*,
29 2006, Wakefield *et al.*, 2011); and in response to changes in oceanographic conditions
30 (Xavier *et al.*, 2013). Ecological niche modelling must be conducted with an awareness of
31 the multi-faceted influences on habitat selection if it is to be informative for identifying and
32 managing priority areas for conservation (Lascelles *et al.*, 2012).

33
34 The energetic demands of reproduction are known to strongly influence habitat selection by
35 pelagic seabirds during breeding periods. The constraints of incubation and chick
36 provisioning impose a central-place foraging mode, as trips are restricted to waters within an
37 accessible range of the colony (Weimerskirch *et al.*, 1993). Individuals face trade-offs

38 between the costs of flight and the necessity for reliable acquisition of prey of sufficient
39 quality to meet the demands of chick provisioning in addition to their own energetic
40 requirements, including for self-maintenance (Weimerskirch *et al.*, 1997). These constraints
41 are particularly pronounced during the brood-guard period, when chicks require continual
42 attendance by a parent to avoid chilling, are at their most vulnerable to predation, and have a
43 small stomach volume so require frequent meals (Weimerskirch *et al.*, 1988, Xavier *et al.*,
44 2003, Wakefield *et al.*, 2011).

45
46 Breeding success is therefore conditional upon the abilities of each bird to predict the
47 locations of suitable foraging habitats within a commutable distance of the colony. The
48 oceanic seascapes over which pelagic seabirds search for food are highly heterogeneous, with
49 prey distributed within a *nested patch hierarchy* (Fauchald *et al.*, 2000, Weimerskirch 2007).
50 Suitable foraging habitats that include prey of sufficient number and quality are accessible
51 within the diving capabilities of the species, are formed by stochastic biophysical processes;
52 hence, the locations of exploitable prey aggregations are usually unpredictable at small spatial
53 scales (Hazen *et al.*, 2013). However, there is evidence to suggest that some species,
54 particularly albatrosses, may target or track regions in which the availability of prey resources
55 is related to persistent oceanographic conditions and hence predictable over broad- to meso-
56 scales, thus optimising foraging success (Kappes *et al.*, 2010, Louzao *et al.*, 2011, Piatt *et al.*,
57 2006, Weimerskirch 2007).

58
59 Grey-headed albatrosses (GHA) *Thalassarche chrysostoma*, in common with many Southern
60 Ocean predators, have been shown to exploit predictable and profitable foraging opportunities
61 generated through bio-physical coupling along ocean fronts – physical interfaces between
62 contrasting water masses (Bost *et al.*, 2009, Belkin *et al.*, 2009). The Antarctic Polar Frontal
63 Zone (APFZ), an extensive, dynamic region that marks the northern boundary of the Antarctic
64 Circumpolar Current (ACC), is known to be an important feature for seabirds and marine
65 mammals in this sector of the Southern Ocean (Catry *et al.*, 2004, Scheffer *et al.*, 2012,
66 Wakefield *et al.*, 2011). Within the broad-scale APFZ, intense oceanographic dynamics lead
67 to the generation of chaotic eddies and the manifestation of mesoscale (10s -100s of
68 kilometres) or sub-mesoscale (~1 kilometre) thermohaline fronts. Aggregations of prey, such
69 as the mesopelagic fish and cephalopods often targeted by the grey-headed albatross, can be
70 concentrated within this zone, both through processes of mechanical entrainment and bottom-
71 up forcing of biophysical hotspots (Rodhouse & White 1995, Reid *et al.*, 1996, Catry *et al.*,
72 2004, Rodhouse & Boyle 2010). Areas of frequent or persistent frontal activity, such as the
73 APFZ, may therefore constitute predictable foraging habitats for regional populations of
74 pelagic seabirds.

75

76 Here, a novel application of EENM is developed, using high-resolution data tracking the
77 movements and activity patterns of GHA from the largest global colony, to identify persistent
78 oceanographic conditions that characterise predictable foraging habitats within the area
79 accessible to breeding birds. We use a suite of remotely-sensed oceanographic data,
80 including the first regional application of a thermal front frequency index, in an iterative
81 presence-availability model framework, with the following aims: i) to identify the biophysical
82 conditions that characterise the locations of observed foraging events during the brood-guard
83 phase; ii) to model the spatial distribution of predictable foraging habitats, iii) to explore the
84 comparative utility of EENM and single-algorithm models in the context of using movement
85 data to define foraging habitats of wide-ranging species over broad- to meso-scales and iv) to
86 evaluate the extrapolative performance of EENM through time, and hence its usefulness for
87 conservation and management applications.

88

89

90 (A) Methods

91

92 (B) Device deployment

93

94 Birds were tracked from Colony B at Bird Island, South Georgia (54°00'S 38°03'W) over
95 December-January of two austral breeding seasons, during the brood-guard phase (total n=55
96 birds; n=25 in 2009/10; n=30 in 2011/12; Fig. 1). GPS loggers used were i-gotU
97 (MobileAction Technology; <http://www.i-gotu.com>; 25g mass), earth & Ocean Technology
98 (e&O-Tec) MiniGPSlog (25g) or e&O-Tec MicroGPSlog (10g) and were attached using
99 Tesa® marine cloth tape (total 5g) to mantle feathers. Devices were programmed to record
100 fixes at 10 or 15 minute intervals and were recovered after one complete foraging trip. Birds
101 were also equipped with geolocation-immersion loggers (British Antarctic Survey; Mk 13;
102 ~1.5g mass), attached to a standard British Trust for Ornithology metal or plastic ring. Birds
103 were restrained on the nest only during device deployment, and handling time during
104 deployment and retrieval was minimised (5-10 mins).

105

106 (B) Behavioural classification

107

108 Landing rate (number of landings per 10-minute interval) derived from the immersion data
109 was used to identify foraging bouts (following Dias *et al.*, 2010). Take-off from the water
110 surface is energetically costly for albatrosses, so we assumed that immersion events indicated
111 prey capture attempts (following Wakefield *et al.*, 2011). Empirical evidence from previous

112 work on this population shows that birds frequently catch prey in rapid directed flight without
113 any obvious area-restricted search (ARS) behaviour (Catry *et al.*, 2004), so we used landing
114 rate as an indicator of foraging behaviour in preference to identifying ARS.

115

116 Locations of immersion events were derived through temporal matching of GPS and
117 immersion data. As birds rest on the water surface overnight (Catry *et al.*, 2004), and night-
118 time foraging could not be differentiated from resting, only those locations recorded in
119 daylight hours were used (bounded by civil dawn and dusk; solar zenith angle of -6°). All
120 locations within a 50km radius of the colony were excluded from analysis to remove rafting
121 behaviour. All GPS tracks were interpolated to regular 10 minute intervals. Landing rate was
122 derived using a sliding window that summed the number of immersion events and total time
123 spent immersed in the 10 minute track section preceding each GPS point location.

124 Interpolated point locations along each track were then classified as either foraging –
125 associated with at least one immersion event within ten minutes – or transit – not associated
126 with immersion.

127

128 The study area was defined as the area enclosing a radius corresponding to the absolute
129 maximum displacement from the colony by any tracked bird (1185km). To obtain an
130 indication of the spatial distribution of foraging events over the tracking period, a 2-
131 dimensional regular grid of the study area (71°S to 32°S ; 55°W to 21°W) was created at 0.5°
132 resolution. A binary classification index of grid cell usage was used to identify foraging areas
133 - grid cells in which foraging events were recorded over the course of the tracking period
134 were designated as 1, and grid cells that contained transit locations, or no bird presence, were
135 designated as 0. All analyses were conducted in R version 3.1.

136

137 (B) Oceanographic data

138

139 Remotely-sensed oceanographic data were obtained for a matching timespan (late December
140 – end January) for each tracking period (2009/10; 2011/12). Daily NASA Multi-Sensor
141 Merged Ultra-High Resolution (MUR) Sea Surface Temperature (SST) imagery was
142 downloaded via OpenDAP, and daily chlorophyll-*a* (chl-*a*) imagery was processed from
143 MODIS-Aqua data; both were mapped to the study area in geographic projection at 1.2km
144 resolution. Daily images were used to generate monthly median SST and chl-*a* (log-scaling)
145 composites. Bathymetric data were obtained for a matching spatial extent from the General
146 Bathymetric Chart of the Oceans (GEBCO_08 grid; <http://www/gebco.net>), and used to
147 derive depth at 30 arc-second resolution.

148

149 Thermal composite front maps (Miller 2009) were generated from MUR SST data, over
150 rolling 7-day periods spanning the tracking period. Thermal fronts were detected in each
151 MUR SST scene using Single-Image Edge Detection (SIED; Cayula & Cornillon 1992; front
152 detection threshold = 0.4°C). Successive 7-day composites were used to prepare monthly
153 front frequency (*TFreq*) layers, which quantify the frequency in which a front is detected in
154 each pixel as a ratio of the number of positive detections to the number of cloud-free
155 observations. All environmental data layers were standardised at 0.5 degree resolution
156 through bilinear interpolation ('raster' package for R; Hijmans & van Etten 2012; Fig. 2).
157 Oceanographic data layers were selected on the basis of availability, coverage and previously
158 demonstrated influence on habitat selection by GHA and sympatric seabird species (e.g.
159 Xavier *et al.*, 2003, Phillips *et al.*, 2006, Wakefield *et al.*, 2011, Ballard *et al.*, 2012).

160

161 (B) Ensemble Ecological Niche Modelling (EENM)

162

163 Previous work comparing the efficacy of various modelling algorithms for predicting habitat
164 preferences in seabirds concluded that an ensemble approach can be preferable to the use of a
165 single-algorithm models (Oppel *et al.*, 2012). However, the technique has not to our
166 knowledge been used previously to identify predictable foraging habitats for seabirds using
167 movement data. We used EENM to identifying the biophysical conditions characterising the
168 locations of observed albatross foraging events. Ecological niche models (ENM) were fitted
169 using the Generalised Additive Modelling (GAM), Maximum Entropy (MaxEnt), Random
170 Forest (RF) and Boosted Regression Tree (BRT) algorithms within the biomod2 package for
171 R (Thuiller *et al.*, 2009, 2014).

172

173 The package 'biomod2' uses a presence-availability framework to model preferred conditions.
174 As grid cells in which no foraging events were detected cannot be classified as true absences,
175 control locations ('pseudo-absences') were iteratively resampled from within the accessible
176 radius of the breeding colony. Five iterations of 1000 randomly-selected control locations
177 were used over successive model runs (Barbet-Massin *et al.*, 2012). Each model run involved
178 10-fold cross-validation, with data randomly apportioned to a 75% / 25% split for model
179 calibration and testing phases.

180

181 Relative importance of environmental variables was determined using the built-in method in
182 biomod2, which overcomes difficulties associated with comparing model-specific outcomes
183 through a randomisation procedure (Thuiller *et al.*, 2009, 2014), which fits a Pearson
184 correlation between the fitted values and predictions, where each variable has been randomly
185 permuted. If the two predictions are similar, i.e. highly correlated, the variable is

186 considered of little importance. This procedure was repeated 10 times for each variable
187 within each model run. The relative importance of each environmental variable (Relative
188 Importance of the Contribution to the model Coefficients, RICC) was then scaled by
189 subtracting the mean correlation coefficient from 1. The overall explanatory power of the
190 environmental variables was derived using the mean-of-means of standardised variable
191 importance over all iterations per algorithm (Table S1).

192

193 The EENM combines predictions from single-algorithm model runs. Outputs of each single-
194 algorithm model were evaluated over both model calibration and testing datasets for each
195 model iteration. A triad of model performance metrics (AUC, TSS, Boyce Index) was
196 generated for each iteration per algorithm, and the mean of each of these metrics over each
197 iteration of control locations was calculated. The mean of each performance metric over all
198 models fit per algorithm was then calculated (n=50; 10-fold cross-validation for each of 5
199 iterations of control locations; Tables S3, S4). Only those with a True Skill Statistic (TSS)
200 equal to or greater than 0.7 were included in the final ensemble, to minimise inclusion of
201 poorly-performing models. The ensemble projections were created using a weighted average
202 across all included single-algorithm models, based on TSS, and accounting for differences in
203 algorithm performance. EENM projections were based on a habitat suitability index (HSI),
204 scaled between 0 and 1, where 1 represents greatest suitability.

205

206 Resultant EENMs were then evaluated, using AUC, TSS and Boyce Index (Boyce *et al.*,
207 2002; Hirzel *et al.*, 2006). We calculated all performance metrics for each EENM fitted to the
208 full dataset from each year. AUC and TSS were calculated using in-built biomod2
209 functionality. Boyce Index was calculated through projection of each model on to the full
210 dataset for each year ('ecospat' package for R; Broenniman *et al.*, 2014) to obtain a value
211 comparing model predictions of HSI with the input presence dataset in each case.

212

213 In preference to specifying a threshold of HSI to calculate the extent of suitable foraging
214 habitat within the area accessible to the population during this breeding phase, we derived a
215 measure of the proportion of this accessible area in which suitable foraging conditions were
216 predicted over a continuum of HSI from 0 to 1.

217

218 (B) EENM Extrapolative Performance

219

220 EENM extrapolative performance was assessed through cross-validation between the two
221 years for which we had data. We projected each model on to the combined synoptic
222 environmental data surfaces for the years following (2009/10 model onto 2011/12

223 environmental data) or preceding (2011/12 model onto 2009/10 environmental data) that upon
224 which the model was constructed. Performance metrics (AUC, TSS, Boyce Index) were
225 calculated for each of these projected models, following methods described above. Spatial
226 concordance between predictions of models extrapolated across time and year-specific
227 models was quantitatively compared using Mantel tests (ade4 package for R; Dray & Dufour,
228 2004).

229

230 (A) Results

231

232 (B) Foraging Trips

233 Maximum displacement from the colony ranged between 153km and 1185km, with a mean \pm
234 SD of 744 ± 249 km. Trip duration ranged between 0.6 and 6.1 days, with a mean of 2.9 ± 1.3
235 days. All trips involved at least one foraging event (based on landing rate derived from the
236 immersion data), with a mean of 6.1 ± 3.7 foraging events per trip (range 2 – 17).

237 Sex was available for a small sub-sample of tracked birds (n=8, 2009/10; n=5, 2011/12), in
238 which no differences in foraging trips between sexes were detected (Fig. 1). Given the small
239 sample of known sex, sex effects were not included in further population-level analyses.

240

241 (B) Predictable foraging habitats

242 Median SST and chl-*a* concentration were important contributory variables to EENMs
243 constructed for both years of the study, suggesting these biophysical variables strongly
244 influence albatross foraging over the scales investigated by our models (Table 1). However,
245 the overall explanatory contribution of chl-*a* to the 2011/12 EENM (RICC=0.150) was lower
246 than its contribution to the 2009/10 EENM (RICC=0.585), and the inverse was observed for
247 the contribution of SST to each EENM (RICC, 2009/10=0.577; RICC, 2011/12=0.744). The
248 relative contributions of water depth and the frequency of mesoscale thermal front
249 manifestation (*TFreq*) to the explanatory capabilities of the EENM were lower than that of
250 SST and chl-*a* across both years, although *TFreq* and depth were more important to the
251 2011/12 model set (RICC, *TFreq*=0.155, RICC, depth=0.100) than for 2009/10 (RICC,
252 *TFreq*=0.037; RICC depth=0.086).

253

254 Spatial predictions of EENMs identified suitable foraging conditions across neritic (<500m
255 depth), shelf-break and oceanic regions, reflecting the variety of foraging locations used by
256 birds tracked in both the 2009/10 and 2011/12 breeding seasons (Fig. 3). EENM-derived
257 spatial predictions of habitat suitability across the accessible area were very similar in extent
258 and direction among years (Fig. 3a,b). Regions of high habitat suitability were associated with
259 particular SST ranges (3-8°C, 12-13°C) and productive regions (median chl-*a* >0.5 mg m⁻³) of

260 the area accessible to foraging birds. The APFZ (Fig. 2e,f) was also identified as an area
261 highly suitable for foraging in both years (Fig. 3), although this zone lies at the extremes of
262 the area accessible to birds during this breeding stage (Fig. 1).

263

264 (B) EENM vs. single-algorithm models

265

266 (C) Model Predictions

267 The ranking of the environmental variables in terms of explanatory contribution (mean over
268 50 runs per algorithm) was broadly comparable among single-algorithm models, although we
269 observed some variability (Table 1). For example, ranking of environmental variable
270 importance was similar among GAM, RF and BRT models in both years. EENM variable
271 rankings smoothed out the variability evident in estimated variable importance among model
272 sets. However, explanatory contributions of environmental variables were ranked differently
273 by year-specific EENMs (Table 1).

274

275 Model response curves for each environmental variable were comparable among algorithms.
276 GAM, RF and BRT in particular generated model sets with very similar response curves for
277 SST (Fig. 4), *TFreq* and depth, although less consistency among algorithms is evident in chl-*a*
278 response curves. MaxEnt models were subject to greater inconsistency in predicted responses
279 (Figs. S1 – S3).

280

281 Similarly, spatial predictions of models fitted using the GAM, RF and BRT algorithms were
282 comparable in the extent and location of suitable habitats identified, and in the scaling of the
283 habitat suitability index (HSI) in these regions (Fig. 5). MaxEnt models, however, generated
284 more spatially restricted predictions with overall lower HSI predicted throughout the
285 accessible area. For these reasons, we did not include MaxEnt in the final EENMs per year.
286 The location and extent of suitable habitats identified and the scaling of HSI in EENM
287 predictions integrated the predictions of the GAM, RF and BRT algorithms, smoothing over
288 variation between model frameworks (Fig. 3). Spatial predictions of all single-algorithm
289 models were similar in extent, location and HSI scaling among years (Fig. 5). EENM
290 predictions showed a strong spatial concordance in the location and extent of suitable habitats
291 identified in each year (Fig. 3; HSI, Mantel $r=0.9599$).

292

293 (C) Model Performance

294 EENMs were highlighted by AUC and Boyce Index as the best performing models in
295 comparison with all single-algorithm models for both years. However, the True Skill Statistic
296 (TSS) selected Random Forest (RF) as the best performing in both years (Table 2).

297

298 Evaluation metrics indicated similar performance of single-algorithm models across model
299 sets, (variance, AUC=0.0002; TSS=0.001; Boyce Index=0.002; Table 2), and for each of
300 these single-algorithm models among years (correlation, AUC $r=0.999$; TSS=0.935; Boyce
301 Index=0.884; Table 2). There was little concordance between the rankings of model
302 performance for single-algorithm models among the three model performance metrics used
303 (AUC, TSS, Boyce Index), although AUC and TSS ranked single-algorithm models in a
304 similar order in both years (e.g. AUC = RF, BRT, GAM, MaxEnt; Table 2).

305

306 The exclusion of MaxEnt models from the final EENMs per year had little effect on model
307 performance metrics, although a slight improvement was evident in AUC, TSS and Boyce
308 Index in both years (Table 2). The weighted mean EENM including predictions of GAM, RF
309 and BRT models was retained as the final model for each year.

310

311 (B) EENM Extrapolative Performance

312

313 EENMs extrapolated across years to predict suitable foraging habitats over differing
314 mesoscale oceanographic conditions performed well according to AUC and Boyce Index
315 scores of projected models. All model performance metrics (AUC, TSS, Boyce Index) reveal
316 the extrapolative performance of the 2011/12 EENM to be superior to that of the 2009/10
317 EENM. However, the TSS scores of both models dropped below the 0.7 threshold used to
318 select best performing models for EENM creation.

319

320 Spatial predictions of EENMs extrapolated across years were broadly comparable to the
321 predictions of each year-specific EENM, highlighting the suitable foraging habitats located to
322 the north and west of the colony. Extrapolation of the 2011/12 EENM to the 2009/10
323 combined environmental data surface exhibited strong similarity with the 2009/10 EENM
324 (HSI, Mantel $r=0.9437$), but extrapolation of the 2009/10 EENM on to 2011/12 conditions
325 predicted more spatially restricted regions of high habitat suitability than those predicted by
326 the year-specific model (HSI, Mantel $r=0.8740$; Fig. 3). The proportion of the area accessible
327 to the population during this breeding phase in which suitable foraging habitats were
328 predicted to occur was also comparable among years (Fig. 6).

329

330 (A) Discussion

331 Predictable foraging habitats for the grey-headed albatross population breeding at Bird Island,
332 South Georgia appear to coincide with a set of persistent biophysical conditions characterised
333 by particular thermal ranges and elevated primary productivity. Over the spatial and temporal

334 scales investigated by our models, EENM performed better than single-algorithm models in
335 predicting the locations of suitable foraging habitats. These insights highlight the potential of
336 EENM as a tool for use with movement data for identifying at-sea habitats of wide-ranging
337 marine predators, with clear implications for conservation and management.

338

339 (B) Predictable foraging habitats

340

341 Our ensemble ecological niche models (EENMs) highlight sea surface temperature (SST) and
342 median surface chlorophyll-*a* (chl-*a*) concentration (monthly synoptic fields) as important
343 determinants of habitat suitability for foraging grey-headed albatrosses during the brood-
344 guard phase. SST has been found to be a useful predictor of habitat preference for other
345 albatross species at South Georgia, and elsewhere (Wakefield *et al.*, 2011; Deppe *et al.*, 2014,
346 Kappes *et al.*, 2010; Awkerman *et al.*, 2005). GHA also appeared to respond to the frequency
347 of mesoscale thermal front manifestation (*Tfreq*), which characterised the APFZ, and to water
348 depth, although these predictors had less influence in models.

349

350 SST is a proxy for the spatial structuring of biophysical conditions over the vast ranges
351 utilised by these ocean-wandering seabirds, and so often proves useful in identifying
352 predictable habitats. Different foraging guilds of pelagic predators exploit prey types that
353 associate with particular temperature regimes (Commins *et al.*, 2014). GHA are known to
354 seize prey from the ocean surface (<2-3m depth; Huin & Prince 1997), and to feed
355 predominantly on ommastrephid squid, including *Martialia hyadesi*, crustaceans, including
356 Antarctic krill *Euphausia superba*, and, less commonly, lamprey *Geotria australis*,
357 mesopelagic fish and gelatinous zooplankton (Rodhouse *et al.*, 1990, Reid *et al.*, 1996, Xavier
358 *et al.*, 2003, Catry *et al.*, 2004). Although the diet of the tracked birds was not determined in
359 the current study, their distribution was broadly comparable with previous years when all
360 these prey types were recorded (Catry *et al.*, 2004, Xavier *et al.*, 2003). This suggests that the
361 environmental conditions identified through this modelling procedure reflect the key habitats
362 and main prey that are targeted by grey-headed albatrosses at South Georgia, which represent
363 c. 50% of the global breeding population (ACAP 2009).

364

365 Chl-*a* was also identified as a predictor of the spatial distribution of foraging events. Overall,
366 foraging activity was more likely in productive regions. Chl-*a* concentrations (monthly
367 median) were highest on-shelf, with peak values recorded to the south-west of the colony.
368 The APFZ was not characterised by elevated productivity over the spatial and temporal scales
369 investigated in this model. Birds foraging in productive shelf waters around South Georgia
370 are likely to be targeting Antarctic krill and icefish *Champscephalus gunnari*, which are

371 more closely tied to bottom-up forcing mechanisms than the squid and mesopelagic fish
372 found in the APFZ (Wakefield, Phillips & Belchier 2012).

373

374 High *Tfreq* values and narrow SST contours characterise the APFZ, which was identified by
375 the EENM as a region of high habitat suitability for GHA. Plunge-diving GHA have been
376 observed in association with large aggregations of *M. hyadesi* at the ocean surface within the
377 APFZ (Rodhouse & Boyle 2010). Although few foraging events were observed in the APFZ
378 during the tracking period, it is likely that those birds foraging in the APFZ region were
379 targeting ommastrephid squid. The APFZ lies at the northernmost extreme of the observed
380 foraging range during brood-guard, which might suggest that reproductive constraints
381 influenced the strength of the association with this region. Regardless, the high spatial
382 overlap between the APFZ and the distribution of GHA during other breeding stages and in
383 the non-breeding period (Phillips et al. 2004, Croxall et al. 2005) suggest it is a key foraging
384 area for this species, year-round.

385

386 In previous studies in the region, the spatial extent of the APFZ has been estimated using
387 historical or averaged data, which did not match the temporal resolution of animal movement
388 data. For example, Xavier *et al.* (2003) used the position of the Polar Front (PF) derived from
389 survey data in 1997 to investigate habitat preference of birds tracked in 2000. However, the
390 APFZ is a highly dynamic feature, characterised by intense mesoscale variability, and the PF
391 can vary in position by as much as 100km in 10 days (Trathan *et al.*, 1997). Detecting fronts
392 in a temporally-averaged SST composite can also mask the dynamic nature of these features.
393 The *Tfreq* index, used here for the first time in the Southern Ocean, is an objective, synoptic
394 product that enables incorporation of mesoscale oceanographic dynamics in broad-scale
395 ecological niche models (Scales *et al.*, 2014).

396

397 In addition to the selection of environmental data layers, analytical scale is a key aspect of the
398 construction of ecological niche models. Matching the spatial resolution of remotely-sensed
399 datasets with the scales over which animals locate key foraging areas remains a major
400 challenge in habitat modelling (Storch 2002, Luoto *et al.*, 2007), particularly in the marine
401 realm (Araújo & Guisan 2006, Hirzel *et al.*, 2006). In our study, environmental data layers
402 were interpolated to a standard 0.5 degree grid resolution, which was deemed appropriate
403 given the extent of the area over which tracked birds roamed. In order to ensure scale match
404 of the research question, response and environmental datasets, we also restricted temporal
405 averaging of environmental data layers to one month, matching the duration of the brood-
406 guard phase for the focal population.

407

408 (B) EENM vs single-algorithm models

409

410 (C) Model Predictions

411 Single-algorithm ecological niche models fitted on the same dataset can perform differently
412 and generate contrasting predictions (Guisan & Zimmerman 2000, Thibaud *et al.*, 2014).

413 Choosing a set of algorithms to fit an EENM is, therefore, central to its predictive capability.

414 Here, several algorithms that are used widely in habitat models for wide-ranging marine
415 vertebrates were combined in an ensemble.

416

417 Single-algorithm models used here ranked the relative importance of environmental variables
418 differently in both years, yet overall concordance was observed in estimated variable
419 importance between algorithms. Relative variable importance in final EENMs for each year
420 broadly echo the consensus in variable ranking among GAM, RF and BRT model sets. Year-
421 specific EENMs conflicted in the ranking of environmental variable importance. SST, *TFreq*
422 and Depth were ascribed greater importance in the 2011/12 ensemble, whereas the importance
423 of chl-*a* dropped from 2009/10 to 2011/12. This could be attributable to non-stationary
424 processes that govern the foraging responses of grey-headed albatrosses to oceanographic
425 conditions over the scales at which our analysis was focused (Jenouvrier *et al.*, 2005), or
426 indicative of the need for additional environmental data to enhance the capacity of our models
427 to sufficiently capture the foraging seascape experienced by this population.

428

429 Concordance in model response curves per environmental variable from single-algorithm
430 models increases confidence in the capacity of these models to detect true responses to
431 environmental conditions. We observed strong concordance between model response curves
432 resulting from GAM, RF and BRT across all environmental variables in both years, and so
433 included these model sets in final EENMs. EENM predictions integrating outputs of several
434 single-algorithm models predicting broadly similar responses could be regarded as preferable
435 to any single-model output in terms of confidence in predictions. Similarly, broadly matching
436 spatial predictions, such as those predicted by GAM, RF and BRT in our analysis, increase
437 confidence in these single-algorithm model outputs, and in the spatial predictions of the final
438 EENMs. This is a key aspect of the utility of the EENM process in enabling the construction
439 of more reliable predictive habitat-based models.

440

441 (C) Model Performance

442 Differences in model performance rankings using alternative metrics (i.e. AUC, TSS, Boyce
443 Index) highlight the potential effect of choice of performance metric on model selection for
444 EENM construction. There is, to our knowledge, no current consensus on which performance

445 metric would be preferable in this context, although the reliability of AUC has been heavily
446 criticised (Boyce *et al.*, 2022; Lobo *et al.*, 2008). The TSS is robust and independent of
447 sample size (prevalence), unlike the commonly used *kappa* statistic (Allouche *et al.*, 2006).
448 As TSS is implemented in the R Package ‘biomod2’ framework, we chose this metric over
449 AUC for model selection for EENM. We also implemented the Boyce Index as a comparative
450 measure of model performance (Boyce *et al.*, 2002; Hirzel *et al.*, 2006). As with all
451 movement datasets, our response variable is strictly presence-only, and so a presence-only
452 model evaluation metric is likely more appropriate than a presence-absence metric such as
453 AUC or TSS. However, we note that the use of multiple performance metrics in EENM
454 construction and evaluation, and comparison between these metrics, is clearly preferable to
455 any single metric (Allouche *et al.*, 2006, Jiménez-Valverde 2012, Thibaud *et al.*, 2014).
456 EENMs were selected as the best performing models in both years using the Boyce Index and
457 AUC methods, indicating that averaging the outputs of several single-algorithm models into
458 an ensemble has improved predictive capacity in our test case.

459

460 Our exploration of the utility of EENM in this context highlights the capacity of the technique
461 for comparing among the predictions of single-algorithm models and selecting the best
462 performing models for a particular dataset or application. A final model can be selected from
463 among the candidate EENMs and single-algorithm outputs. For example, taking a
464 conservative approach, we excluded MaxEnt from final EENMs, improving performance and
465 increasing confidence in predictions. EENM is useful for excluding strong bias and
466 smoothing over weaker biases in different model predictions. Our results exemplify the
467 potential of EENM for use with movement data in identifying predictable foraging habitats
468 for wide-ranging marine vertebrates over broad scales.

469

470 (B) EENM Extrapolative Performance

471

472 Ecological niche models constructed and validated over the same spatial and temporal extent
473 can show limited transferability in space and time (Randin *et al.*, 2006, Torres *et al.*, 2015).
474 While we did not have sufficient movement data to investigate transferability through space,
475 the extrapolative performance of our EENMs across the two years of this study was generally
476 good, although the 2011/12 ensemble performed better than that built for 2009/10 (2009/10,
477 AUC=0.9107, TSS=0.5194, Boyce Index=0.8536; 2011/12, AUC=0.9281, TSS=0.6630,
478 Boyce Index=0.9348). Changes in the performance of ensembles extrapolated across years are
479 indicative of poor transferability through time, because of variation in animal-environment

480 interactions or, more probably, the failure of models to fully capture the drivers of these
481 interactions.

482

483 Further tests of EENM extrapolative performance through space and time, for example to
484 other populations of the same species (e.g. Torres *et al.*, 2015), or through multiple years in
485 the same region, are necessary to ascertain true extrapolative capabilities. Moreover, the
486 multi-scale periodicity of oceanographic variability in the region (e.g. decadal-scale Southern
487 Ocean Oscillation Index) is likely to influence extrapolative capabilities (e.g. Jenouvrier *et al.*,
488 2005). Some key questions remain: for example, after how many years is the extrapolative
489 performance of a year-specific model likely to fade? How do predictable habitats over
490 decadal timescales align with predictable habitats on inter-annual timescales? Future work
491 should investigate the degree of variability within and between years in prevailing
492 oceanographic conditions and preferred foraging areas if these techniques are to prove
493 valuable for predicting population-level responses to climate-driven ecosystem change.

494

495 Nevertheless, ensemble ecological niche models (EENMs) can incorporate differing
496 predictions from species-habitat models fitted using alternative algorithms, where they are
497 implemented with awareness of technical limitations (Marmion *et al.*, 2009, Oppel *et al.*,
498 2012). By better incorporating uncertainty, the output of EENMs provide a robust basis for
499 recommendations relating to the conservation and management of marine vertebrate
500 populations, particularly those of conservation concern

501

502 (A) Acknowledgements

503 We are grateful to the fieldworkers who assisted with the tracking studies at Bird Island. The
504 authors thank Drs. Stephen C. Votier and Beth Scott for useful discussions. This study
505 represents a contribution to the Ecosystems component of the British Antarctic Survey Polar
506 Science for Planet Earth Programme, funded by the Natural Environment Research Council.

507

508 (A) References

- 509 Awkerman, J.A., Fukuda, A., Higuchi, H., & Anderson, D.J. (2005). Foraging activity and
510 submesoscale habitat use of waved albatrosses *Phoebastria irrorata* during chick-
511 brooding period. *Marine Ecology Progress Series*, **291**, 289-300.
- 512 Agreement on the Conservation of Albatrosses and Petrels (ACAP. (2009). ACAP Species
513 assessment: Grey-headed Albatross *Thalassarche chrysostoma*. Downloaded from
514 <http://www.acap.aq> on 17 November 2014

515 Allouche O., Tsoar A., Kadmon R. (2006) Assessing the accuracy of species distribution
516 models: prevalence, kappa and the true skill statistic (TSS). *Journal of Applied*
517 *Ecology* **43**, 1223-1232

518 Araújo M.B., Guisan A. (2006) Five (or so) challenges for species distribution modelling.
519 *Journal of Biogeography* **33**, 677-1688

520 Araújo M.B., New M. (2007) Ensemble forecasting of species distributions. *Trends in*
521 *Ecology & Evolution* **22**, 42-47

522 Ballard G., Jongsomjit D., Veloz S.D., Ainley D.G. (2012) Coexistence of mesopredators in
523 an intact polar ocean ecosystem: The basis for defining a Ross Sea marine protected
524 area. *Biological Conservation* **156**, 72-82

525 Barbet-Massin, M., et al. (2012). Selecting pseudo-absences for species distribution models:
526 how, where and how many? *Methods in Ecology and Evolution* **3**, 327-338

527 Belkin I.M., Cornillon P.C., Sherman K. (2009) Fronts in large marine ecosystems. *Progress*
528 *in Oceanography* **81**, 223-236

529 Bost C.A., Cotté C., Bailleul F., Cherel Y., Charrassin J.B., Guinet C., Ainley D.G.,
530 Weimerskirch H. (2009) The importance of oceanographic fronts to marine birds and
531 mammals of the southern oceans. *Journal of Marine Systems* **78**, 363-376

532 Broenniman O., Petitpierre B., Randin C., Engler R., Breiner F., D'Amen M., Pellissier L.,
533 Pottier J., Pio D., Garcia Mateo R., Di Colla V., Hordijk W., Dubuis A., Scheerer D.,
534 Salamin N., Guisan A. (2014) ecospat: Spatial ecology miscellaneous methods. R
535 package version 1.0.

536 Catry P., Phillips R.A., Phalan B., Silk J.R.D., Croxall J.P. (2004) Foraging strategies of grey-
537 headed albatrosses *Thalassarche chrysostoma*: integration of movements, activity and
538 feeding events. *Marine Ecology Progress Series* **280**, 261-273

539 Cayula J.-F., Cornillon P.C. (1992) Edge detection algorithm for SST images. *Journal of*
540 *Atmospheric and Oceanic Technology* **9**, 67-80

541 Commins M.L., Anson I., Ryan P.G. (2014) Multi-scale factors influencing seabird
542 assemblages in the African sector of the Southern Ocean. *Antarctic Science* **26**, 38-48

543 Croxall, J.P., Silk, J.R.D., Phillips, R.A., Afanasyev, V. and Briggs, D.R. (2005) Global
544 circumnavigations: tracking year-round ranges of non-breeding albatrosses. *Science*
545 **307**, 249-250.

546 Deppe L., McGregor K.F., Tomasetto F., Briskie J.V., Scofield R.P. (2014) Distribution and
547 predictability of foraging areas in breeding Chatham albatrosses *Thalassarche*
548 *eremita* in relation to environmental characteristics. *Marine Ecology Progress Series*
549 **498**:287-301

550 Dias M.P., Granadeiro J.P., Phillips R.A., Alonso H., Catry P. (2010) Breaking the routine:
551 individual Cory's shearwaters shift winter destinations between hemispheres and
552 across ocean basins. *Proceedings of the Royal Society B: Biological Sciences*,
553 rspb20102114

554 Dray, S & Dufour, A.B. (2007) The ade4 package: implementing the duality diagram for
555 ecologists. *Journal of Statistical Software* **22**, 1-20.

556 Fauchald P., Erikstad K.E., Skarsfjord H. (2000) Scale-dependent predator-prey interactions:
557 the hierarchical spatial distribution of seabirds and prey. *Ecology* **81**, 773-783

558 Guisan A., Zimmerman N.E. (2000) Predictive habitat distribution models in ecology.
559 *Ecological Modelling* **135**, 147-186

560 Hazen, E.L., Suryan, R.M., Santora, J.A., Bograd, S.J., Watanuki, Y., & Wilson, R.P. (2013).
561 Scales and mechanisms of marine hotspot formation. *Marine Ecology Progress Series*,
562 **487**, 177-183.

563 Hijmans R.J., van Etten J. (2012) raster: Geographic analysis and modelling with raster data.
564 R package version 20-08 <http://CRAN.R-project.org/package=raster>

565 Hirzel A.H., Le Lay G., Helfer V., Randin C., Guisan A. (2006) Evaluating the ability of
566 habitat suitability models to predict species presences. *Ecological Modelling* **199**,
567 142-152

568 Howell, E. A., Hoover, A., Benson, S. R., Bailey, H., Polovina, J. J., Seminoff, J. A., &
569 Dutton, P. H. (2015). Enhancing the TurtleWatch product for leatherback sea turtles,
570 a dynamic habitat model for ecosystem-based management. *Fisheries Oceanography*.

571 Huin N., Prince P. (1997) Diving behaviour of the grey-headed albatross. *Antarctic Science* **9**,
572 243-249

573 Jenouvrier S., Weimerskirch H., Barbraud C., Park Y. H., Cazelles B. (2005) Evidence of a
574 shift in the cyclicity of Antarctic seabird dynamics linked to climate. *Proceedings of*
575 *the Royal Society of London B: Biological Sciences*, **272**(1566), 887-895.

576 Jiménez-Valverde A. (2012) Insights into the area under the receiver operating characteristic
577 curve (AUC) as a discrimination measure in species distribution modelling. *Global*
578 *Ecology and Biogeography* **21**, 498-507

579 Joiris C.R., Dochy O. (2013) A major autumn feeding ground for fin whales, southern fulmars
580 and grey-headed albatrosses around the South Shetland Islands, Antarctica. *Polar*
581 *Biology* **36**, 1649-1658

582 Kappes, M.A., Shaffer, S.A., Tremblay, Y., Foley, D.G., Palacios, D.M., Robinson, P.W.,
583 Bograd, S.J. & Costa, D.P. (2010). Hawaiian albatrosses track interannual variability
584 of marine habitats in the North Pacific. *Progress in Oceanography*, **86**(1), 246-260.

585 Lascelles, B.G., Langham, G.M., Ronconi, R.A. & Reid, J.B. (2012) From hotspots to site
586 protection: Identifying Marine Protected Areas for seabirds around the globe.
587 *Biological Conservation*, **156**, 5-14.

588 Lobo J.M., Jiménez-Valverde A., Real R. (2008) AUC: a misleading measure of the
589 performance of predictive distribution models. *Global Ecology and Biogeography* **17**,
590 145-151

591 Louzao M., Pinaud D., Peron C., Delord K., Wiegand T., Weimerskirch H. (2011)
592 Conserving pelagic habitats: seascape modelling of an oceanic top predator. *Journal*
593 *of Applied Ecology* **48**, 121-132

594 Luoto M., Virkkala R., Heikkinen R.K. (2007) The role of land cover in bioclimatic models
595 depends on spatial resolution. *Global Ecology and Biogeography* **16**, 34-42

596 Marmion M., Parviainen M., Luoto M., Heikkinen R.K., Thuiller W. (2009) Evaluation of
597 consensus methods in predictive species distribution modelling. *Diversity and*
598 *Distributions* **15**, 59-69

599 Miller P. (2009) Composite front maps for improved visibility of dynamic sea-surface
600 features on cloudy SeaWiFS and AVHRR data. *Journal of Marine Systems* **78**, 327-
601 336

602 Nel D.C., Lutjeharms J.R.E., Pakhomov E.A., Ansorge I.J., Ryan P.G., Klages N.T.W. (2001)
603 Exploitation of mesoscale oceanographic features by grey-headed albatross
604 *Thalassarche chrysostoma* in the southern Indian Ocean. *Marine Ecology Progress*
605 *Series* **217**, 15-26

606 Oppel S., Meirinho A., Ramírez I., Gardner B., O'Connell A.F., Miller P.I., Louzao M.
607 (2012) Comparison of five modelling techniques to predict the spatial distribution and
608 abundance of seabirds. *Biological Conservation* **156**, 94-104

609 Patrick S.C., Weimerskirch H. (2014) Consistency pays: sex differences and fitness
610 consequences of behavioural specialization in a wide-ranging seabird. *Biology Letters*
611 **10**, 20140630

612 Phillips R.A., Silk J.R.D., Phalan B., Catry P., Croxall J.P. (2004) Seasonal sexual
613 segregation in two *Thalassarche* albatross species: competitive exclusion,
614 reproductive role specialization or foraging niche divergence? *Proceedings of the*
615 *Royal Society of London Series B: Biological Sciences* **271**, 1283-1291

616 Phillips R.A., Silk J.R., Croxall J.P., Afanasyev V., Bennett V.J. (2005) Summer distribution
617 and migration of nonbreeding albatrosses: individual consistencies and implications
618 for conservation. *Ecology* **86**, 2386-2396

619 Phillips R.A., Silk J.R., Croxall J.P., Afanasyev V. (2006) Year-round distribution of white-
620 chinned petrels from South Georgia: relationships with oceanography and fisheries.
621 *Biological Conservation* **129**, 336-347

622 Piatt J.F., Wetzel J., Bell K., DeGange A.R., Balogh G.R., Drew G.S., Geernaert T., Ladd C.,
623 Byrd G.V. (2006) Predictable hotspots and foraging habitat of the endangered short-
624 tailed albatross (*Phoebastria albatrus*) in the North Pacific: Implications for
625 conservation. *Deep Sea Research Part II: Topical Studies in Oceanography* **53**, 387-
626 398

627 Pikesley S.K., Maxwell S.M., Pendoley K., Costa D.P., Coyne M.S., Formia A., Godley B.J.,
628 Klein W., Makanga-Bahouna J., Maruca S., Ngouesso S., Parnell R.J., Pemo-
629 Makaya E., Witt M.J. (2013) On the front line: integrated habitat mapping for olive
630 ridley sea turtles in the southeast Atlantic. *Diversity and Distributions* **19**, 1518-1530

631 Randin C.F., Dirnböck T., Dullinger S., Zimmermann N.E., Zappa M., Guisan A. (2006) Are
632 niche-based species distribution models transferable in space? *Journal of*
633 *Biogeography* **33**, 1689-1703

634 Raymond, B., Lea, M.A., Patterson, T., Andrews-Goff, V., Sharples, R., Charrassin, J.B.,
635 Cottin, M., Emmerson, L., Gales, N., Gales, R., Goldsworthy, S.D., Harcourt, R.,
636 Kato, A., Kirkwood, R., Lawton, K., Ropert-Coudert, Y., Southwell, C., ven den Hoff,
637 J., Wienecke, B., Woehler, E.J., Wotherspoon, S. & Hindell, M. A. (2015). Important
638 marine habitat off east Antarctica revealed by two decades of multi-species predator
639 tracking. *Ecography* **38**, 121-129

640 Reid K., Croxall J., Prince P. (1996) The fish diet of black-browed albatross *Diomedea*
641 *melanophris* and grey-headed albatross *D. Chrysostoma* at South Georgia. *Polar*
642 *Biology* **16**, 469-477

643 Rodhouse P., Prince P., Clarke M., Murray A. (1990) Cephalopod prey of the grey-headed
644 albatross *Diomedea chrysostoma*. *Marine Biology* **104**, 353-362

645 Rodhouse P.G., Boyle P.R. (2010) Large aggregations of pelagic squid near the ocean surface
646 at the Antarctic Polar Front, and their capture by grey-headed albatrosses. *ICES*
647 *Journal of Marine Science* **67**, 1432-1435

648 Rodhouse P.G., White M.G. (1995) Cephalopods occupy the ecological niche of epipelagic
649 fish in the Antarctic Polar Frontal Zone. *The Biological Bulletin* **189**, 77-80

650 Scales, K.L., Miller, P.I., Embling, C.B., Ingram, S.N., Pirota, E., & Votier, S.C. (2014).
651 Mesoscale fronts as foraging habitats: composite front mapping reveals
652 oceanographic drivers of habitat use for a pelagic seabird. *Journal of The Royal*
653 *Society Interface*, **11**(100), 20140679

654 Scheffer, A., Bost, C.A., & Trathan, P.N. (2012). Frontal zones, temperature gradient and
655 depth characterize the foraging habitat of king penguins at South Georgia. *Marine*
656 *Ecology Progress Series*, **465**, 281-297.

657 Storch I. (2002) On spatial resolution in habitat models: can small-scale forest structure
658 explain capercaillie numbers? *Conservation Ecology* **6**, 6

659 Thibaud E., Petitpierre B., Broennimann O., Davison A.C., Guisan A. (2014) Measuring the
660 relative effect of factors affecting species distribution model predictions. *Methods in*
661 *Ecology and Evolution* **5**, 947-955

662 Thuiller, W., Lafourcade, B., Engler, R., & Araújo, M. B. (2009). BIOMOD—a platform for
663 ensemble forecasting of species distributions. *Ecography*, **32**(3), 369-373.

664 Thuiller W., Georges D., Engler R. (2014) biomod2: Ensemble platform for species
665 distribution modeling. R package version 3.1-64. [http://CRAN.R-](http://CRAN.R-project.org/package=biomod2)
666 [project.org/package=biomod2](http://CRAN.R-project.org/package=biomod2)

667 Torres L.G., Sutton P., Thompson D.R., Delord K., Weimerskirch H., Sagar P.M., Sommer E.,
668 Dilley B.J., Ryan P.G., Phillips R.A. (2015) Poor transferability of species
669 distribution models for a pelagic predator, the Grey Petrel, indicates contrasting
670 habitat preferences across ocean basins. *PLoS ONE* **10**(3): e0120014. doi:
671 10.1371/journal.pone.0120014

672 Trathan P., Brandon M., Murphy E. (1997) Characterization of the Antarctic Polar Frontal
673 Zone to the north of South Georgia in summer 1994. *Journal of Geophysical*
674 *Research: Oceans (1978–2012)* **102**, 10483-10497

675 Wakefield E.D., Phillips R.A., Trathan P.N., Arata J., Gales R., Huin N., Robertson G.,
676 Waugh S.M., Weimerskirch H., Matthiopoulos J. (2011) Habitat preference,
677 accessibility, and competition limit the global distribution of breeding Black-browed
678 Albatrosses. *Ecological Monographs* **81**, 141-167

679 Wakefield, E.D., Phillips, R.A. & Belchier, M. (2012) Foraging black-browed albatrosses
680 target waters overlaying moraine banks-a consequence of upward benthic-pelagic
681 coupling? *Antarctic Science*, **24**, 269-280.

682 Weimerskirch H. (2007) Are seabirds foraging for unpredictable resources? *Deep Sea*
683 *Research Part II: Topical Studies in Oceanography* **54**, 211-223

684 Weimerskirch H., Bartle J.A., Jouventin P., Stahl J.C. (1988) Foraging ranges and partitioning
685 of feeding zones in three species of southern albatrosses. *Condor* **90**, 214-219

686 Weimerskirch H., Mougey T., Hindermeier X. (1997) Foraging and provisioning strategies of
687 black-browed albatrosses in relation to the requirements of the chick: natural
688 variation and experimental study. *Behavioral Ecology* **8**, 635

- 689 Weimerskirch H., Salamolard M., Sarrazin F., Jouventin P. (1993) Foraging strategy of
690 wandering albatrosses through the breeding season: a study using satellite telemetry.
691 *The Auk* **110**:325-342
- 692 Xavier J., Croxall J., Trathan P., Wood A. (2003) Feeding strategies and diets of breeding
693 grey-headed and wandering albatrosses at South Georgia. *Marine Biology* **143**, 221-
694 232
- 695 Xavier J., Louzao M., Thorpe S., Ward P., Hill C., Roberts D., Croxall J.P., Phillips R.A.
696 (2013) Seasonal changes in the diet and feeding behaviour of a top predator indicate a
697 flexible response to deteriorating oceanographic conditions. *Marine Biology* **160**,
698 1597-1606

699 **Biosketch**

700 This research was carried out by an inter-disciplinary team of authors from multiple
701 institutions, each with expertise in linking animal movements and behaviours to
702 oceanographic conditions in dynamic marine systems. Author contributions: K.S., P.M.,
703 R.P & S.I. conceived the ideas; R.P. collected the tracking data; K.S. and P.M. prepared the
704 remotely-sensed data; K.S. analysed the data and led manuscript preparation; P.M.,E.H.,
705 S.B. and R.P. contributed to manuscript preparation and edits.

Figures & Tables

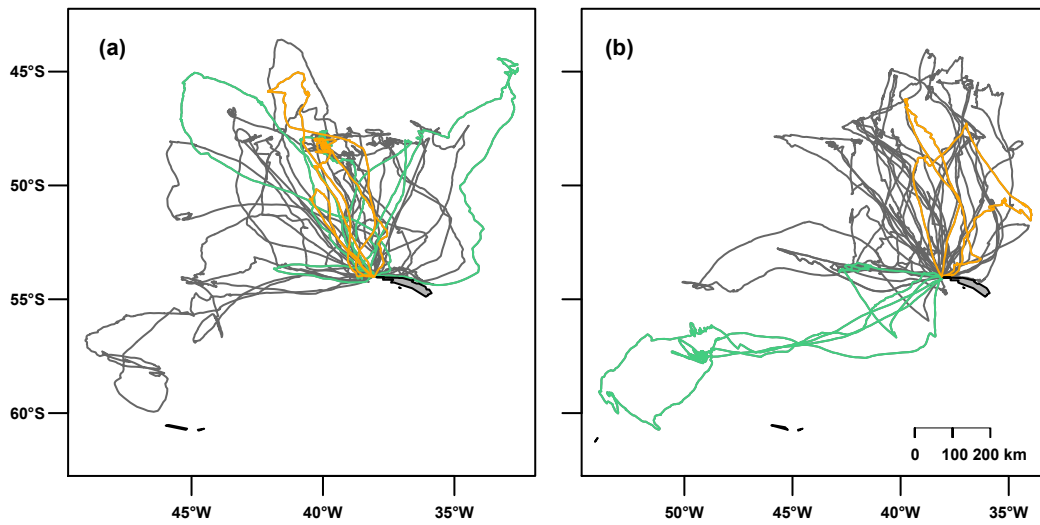


Figure 1 GPS tracking of grey-headed albatrosses (GHA) from Bird Island, South Georgia. Trips used to identify the spatial distribution of foraging events during the (a) 2009/10 (n=25) and (b) 2011/12 (n=30) breeding seasons (brood-guard phase). Birds for which sexes are known are highlighted in orange for female (n=3, 2009/10, n=2, 2011/12) and green for male (n=5, 2009/10; n=3, 2011/12).

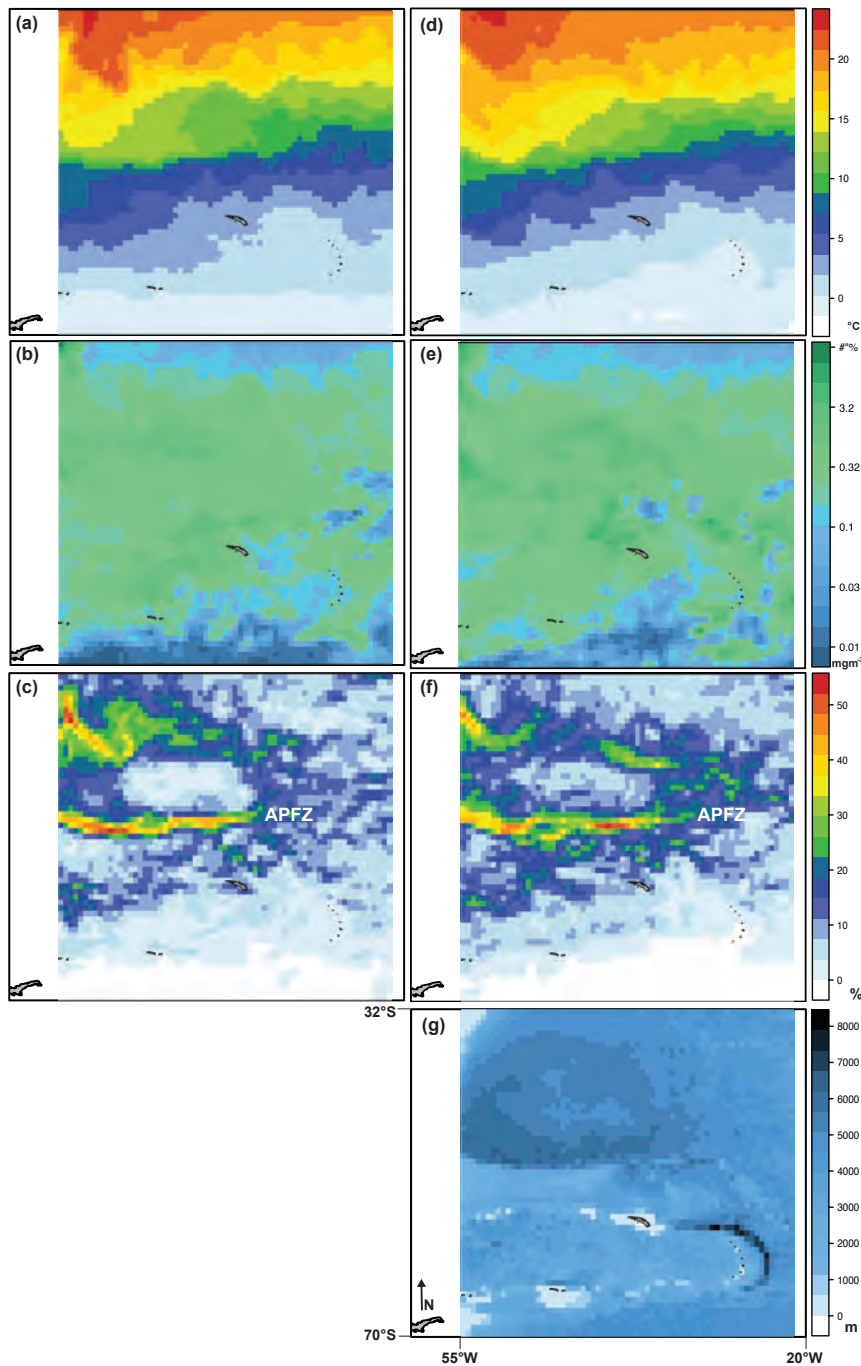


Figure 2 Environmental data layers for brood-guard period (end December – end January). Dynamic variables, (a) Sea Surface Temperature (SST, °C; monthly median composite) for 2009/10, (b) Chlorophyll-a (chl-a, mg m⁻³; monthly median composite; log-transformed), for 2009/10 (c) Thermal front frequency (Tfreq, % time; 0.4°C front detection threshold; monthly synoptic composite) for 2009/10. (d)-(f) Dynamic variables for 2011/12. (g) GEBCO Depth (30 arc-second resolution).

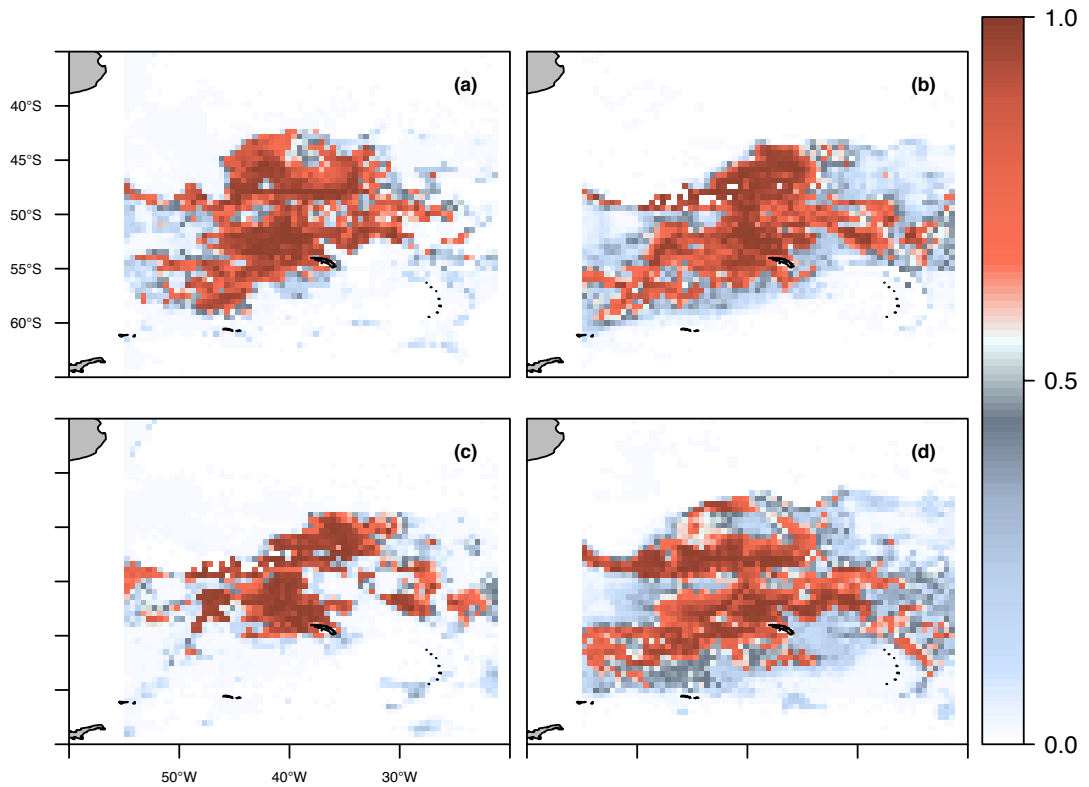


Figure 3 Spatial predictions of ensemble ecological niche models (EENMs), and cross-validation among years. Spatial predictions of final EENM (weighted mean, removal of MaxEnt predictions) for (a) 2009/10 and (b) 2011/12. Cross-validation of (c) 2009/10 EENM onto 2011/12 environmental conditions and (d) 2011/12 EENM onto 2009/10 environmental conditions. Spatial predictions displayed as Habitat Suitability Index (HSI) per grid cell, scaled from 0 to 1. Greater similarity between (a), (b) and (c),(d) indicates better EENM transferability among years.

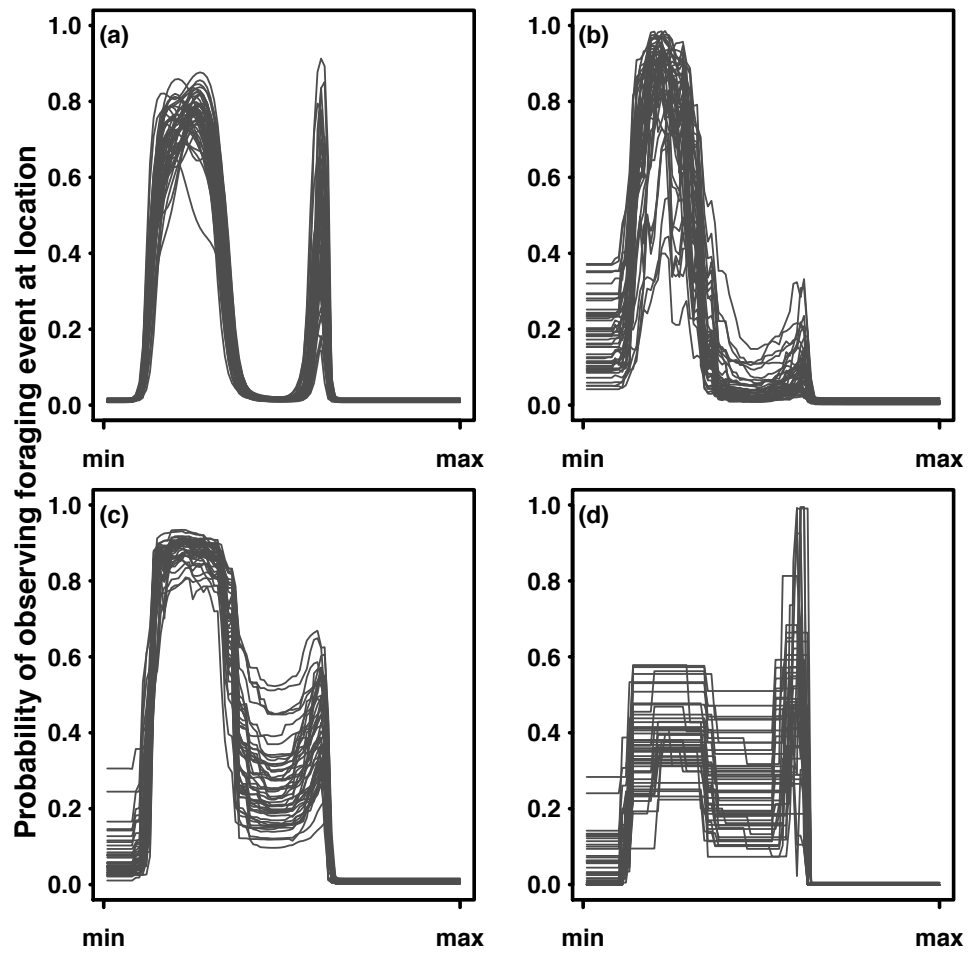


Figure 4 Model Response Curves for SST in 2011/12 model sets, per algorithm, (a) GAM, (b) RF, (c) BRT, (d) MaxEnt

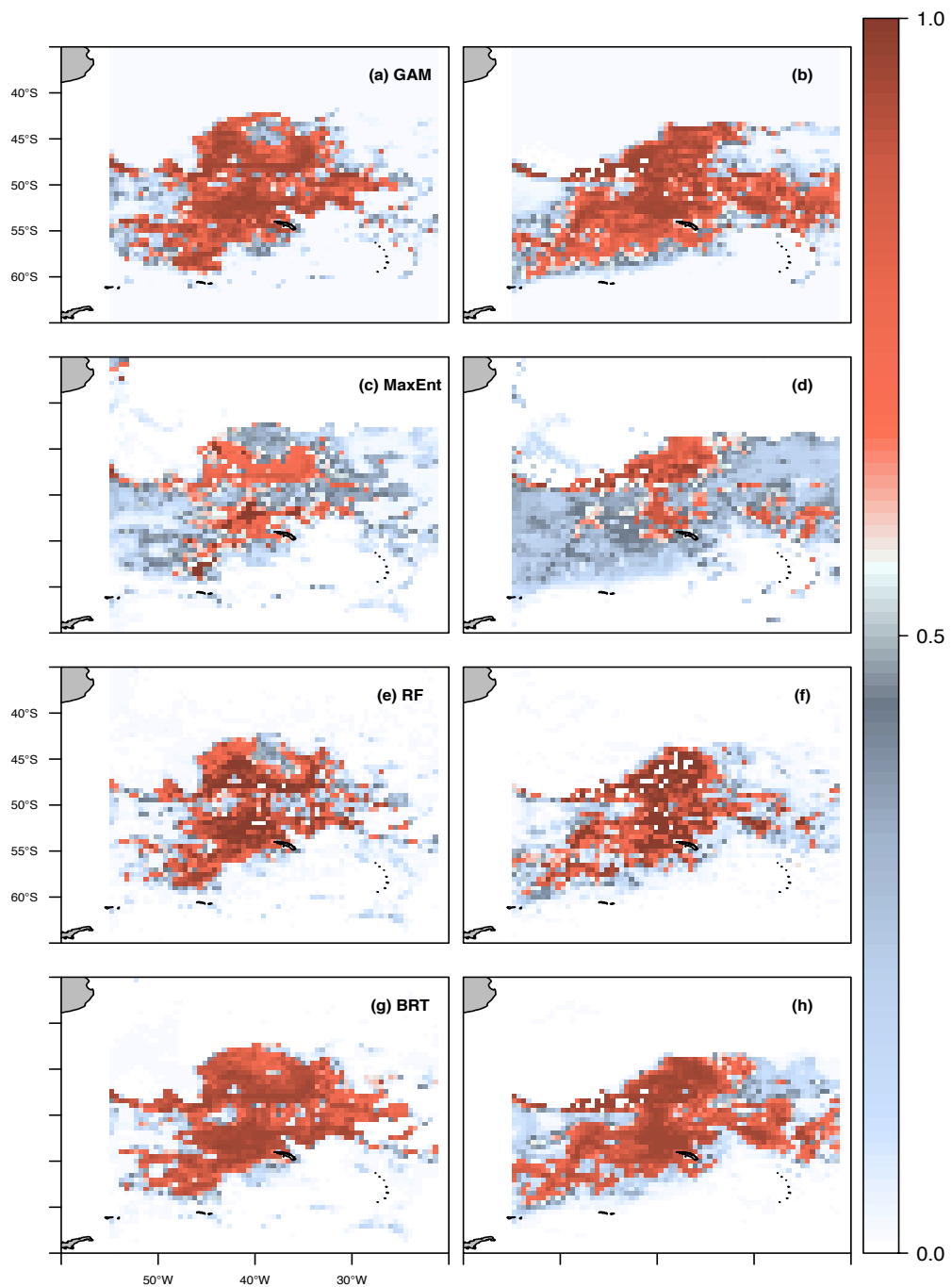


Figure 5 Spatial predictions of ecological niche models per algorithm, (a) Generalised Additive Models, GAM, 2009-10 (b) GAM, 2011/12; (c) Maximum Entropy, MaxEnt, 2009/10, (d) 2011/12; (e) Random Forest, 2009/10, (f) 2011/12; (g) Boosted Regression Trees, 2009/10, (h) 2011/12. Spatial predictions displayed as Habitat Suitability Index (HSI) per grid cell, scaled from 0 to 1 (mean over all model runs, n=50 per algorithm).

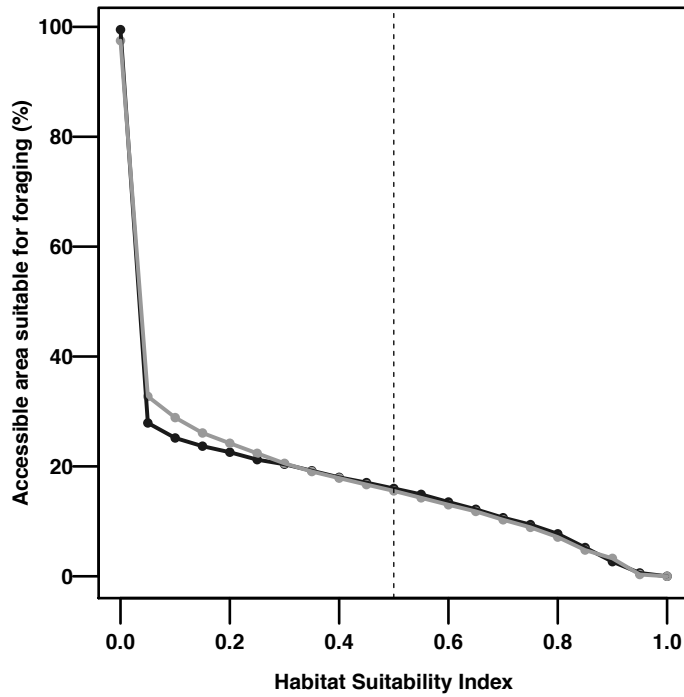


Figure 6 Percentage of area accessible during brood-guard phase (estimated using whole-dataset maximum displacement from colony) containing oceanographic conditions suitable for foraging against EENM-predicted Habitat Suitability Index (HSI). 2009/10 EENM (weighted mean) as black line; 2011/12 in grey.

Figure S1 Model Response Curves for Chl-*a* in 2011/12 model sets, per algorithm, (a) GAM, (b) RF, (c) BRT, (d) MaxEnt

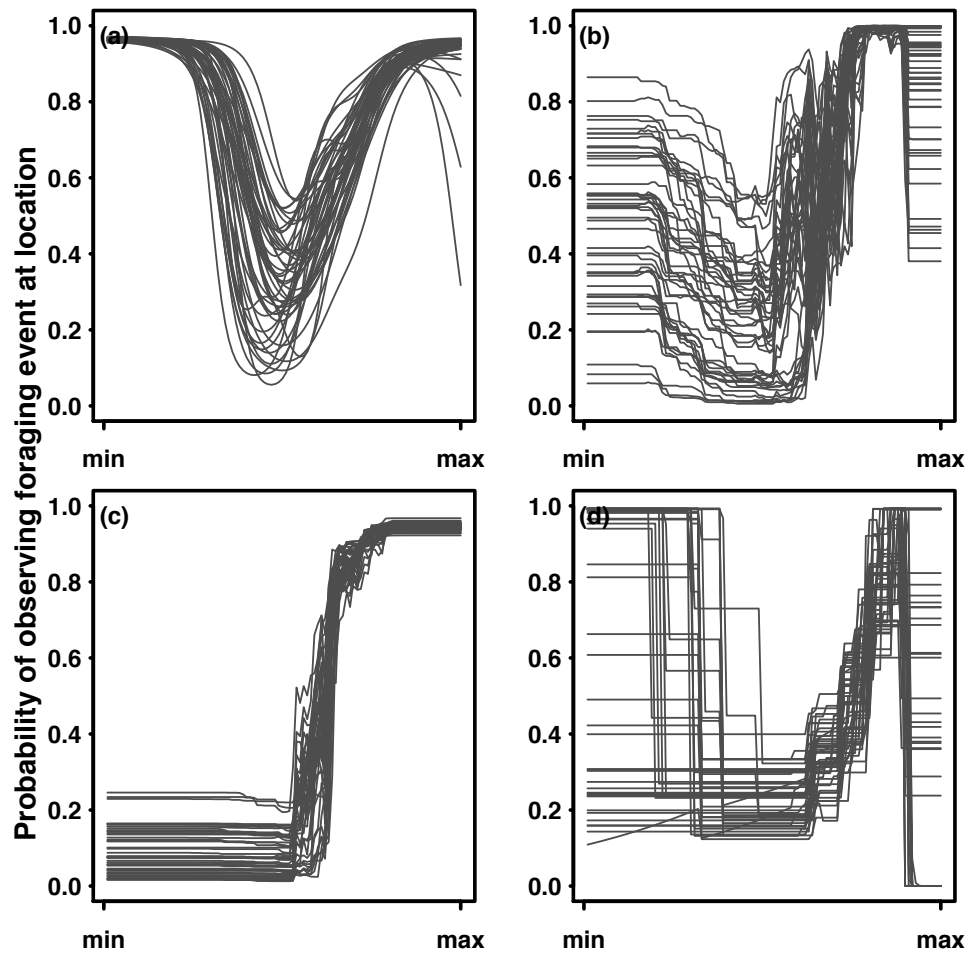


Figure S2 Model Response Curves for *TFreq* in 2011/12 model sets, per algorithm, (a) GAM, (b) RF, (c) BRT, (d) MaxEnt

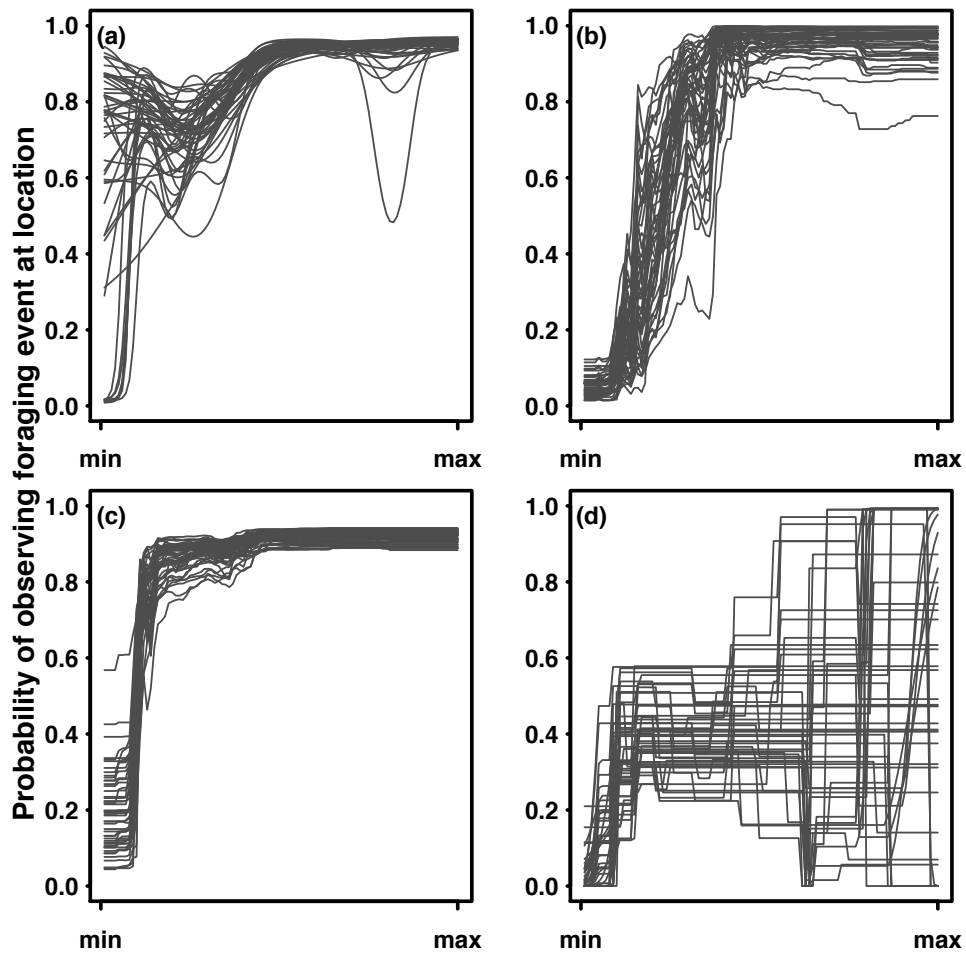


Figure S3 Model Response Curves for depth in 2011/12 model sets, per algorithm, (a) GAM, (b) RF, (c) BRT, (d) MaxEnt

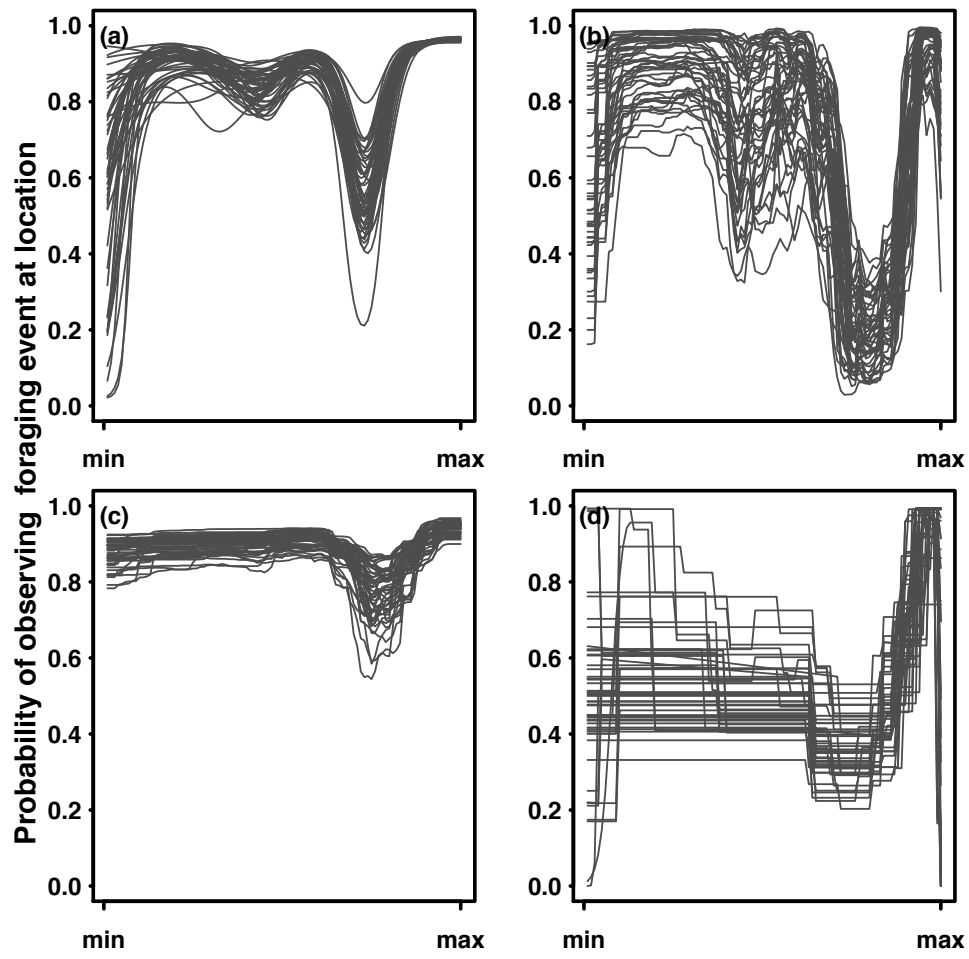


Table 1 Variable Importance (Mean over all model sets per algorithm), scaled as Relative Importance of Contribution to model Coefficients (RICC), from 0 to 1. Variable importance rankings in brackets

	Variable Importance, 2009/10				Variable Importance, 2011/12			
	SST	Chl- <i>a</i>	TFreq	Depth	SST	Chl- <i>a</i>	TFreq	Depth
GAM	0.61396 (1)	0.4570 (2)	0.06512 (4)	0.17284 (3)	0.92174 (1)	0.09860 (3)	0.07752 (4)	0.16574 (2)
MaxEnt	0.45498 (2)	0.48992 (1)	0.06060 (4)	0.12338 (3)	0.55658 (1)	0.21478 (3)	0.31830 (2)	0.18928 (4)
RF	0.46120 (2)	0.52012 (1)	0.08466 (4)	0.16598 (3)	0.51792 (1)	0.27812 (2)	0.24914 (3)	0.20358 (4)
BRT	0.5644 (1)	0.56014 (2)	0.01672 (4)	0.05316 (3)	0.59350 (1)	0.29776 (2)	0.22872 (3)	0.0805 (4)
EENM	0.577 (2)	0.585 (1)	0.037 (4)	0.086 (3)	0.744 (1)	0.150 (3)	0.155 (2)	0.100 (4)

Table 2 Model Performance Metrics (Mean over all model sets per algorithm). Area Under Receiver Operating Characteristic Curve (AUC) scaled 0 to 1; True Skill Statistic (TSS) scaled 0 to 1; Boyce Index scaled -1 to +1. Highest-scoring model for each performance metric highlighted in bold. EENM rows have metrics for final EENM, without MaxEnt (black) and EENM with MaxEnt (grey). Performance rankings per metric in brackets.

	Model Evaluation, 2009/10			Model Evaluation, 2011/12		
Model Set	AUC	TSS	Boyce Index	AUC	TSS	Boyce Index
GAM	0.9421 (3)	0.8237 (2)	0.9213 (2)	0.9372 (3)	0.7835 (3)	0.8943 (3)
MaxEnt	0.9276 (4)	0.7740 (4)	0.9300 (1)	0.9101 (4)	0.7184 (4)	0.9051 (1)
RF	0.9523 (1)	0.8277 (1)	0.8329 (3)	0.9563 (1)	0.8283 (1)	0.8998 (2)
BRT	0.9444 (2)	0.8176 (3)	0.7130 (4)	0.9418 (2)	0.7843 (2)	0.8615 (4)
EENM	0.9547	0.7914	0.9512	0.9610	0.7871	0.9656
	0.9479	0.7514	0.8990	0.9591	0.7791	0.9626
EENM Extrapolation	0.9107	0.5194	0.8536	0.9281	0.6630	0.9358
	0.9038	0.5188	0.7138	0.9267	0.6208	0.9540

Table S1 Variable importance per iteration of control locations, 2009/10. Mean importance of environmental variables (Sea Surface Temperature, SST; Chlorophyll-a, chl-a; thermal front frequency, Tfreq; depth) over model runs (10-fold cross-validation) per iteration of control locations, for each model algorithm (Generalised Additive Models, GAM; Maximum Entropy modelling, MaxEnt; Random Forest, RF; Boosted Regression Trees, BRT). Mean of Relative Importance to the model Coefficients (RICC) metric over successive iteration of control locations.

Control Location Iteration	Model Algorithm	Variable Importance (mean over 10 runs per pseudo-absence iteration)			
		SST	Chl- <i>a</i>	TFreq	Depth
1	GAM	0.6160	0.4646	0.0721	0.1762
	MaxEnt	0.4840	0.5192	0.0784	0.1140
	RF	0.4746	0.5360	0.1122	0.1285
	BRT	0.5679	0.5618	0.0139	0.0396
2	GAM	0.6089	0.4589	0.0690	0.1503
	MaxEnt	0.4779	0.4031	0.1327	0.2149
	RF	0.4523	0.5474	0.0694	0.1651
	BRT	0.5808	0.5655	0.0146	0.0447
3	GAM	0.5992	0.4509	0.0430	0.1572
	MaxEnt	0.4449	0.4771	0.0345	0.1019
	RF	0.4645	0.5094	0.0891	0.1683
	BRT	0.5559	0.5690	0.0244	0.0417
4	GAM	0.6040	0.4803	0.0910	0.1544
	MaxEnt	0.3937	0.5321	0.0364	0.0852
	RF	0.4614	0.5267	0.0743	0.1499
	BRT	0.5470	0.5718	0.0131	0.0544
5	GAM	0.6417	0.4303	0.0505	0.2261
	MaxEnt	0.4744	0.5181	0.0210	0.1009
	RF	0.4532	0.4811	0.0783	0.2181
	BRT	0.5704	0.5326	0.0176	0.0854
mean of means	GAM	0.61396	0.4570	0.06512	0.17284
	MaxEnt	0.45498	0.48992	0.06060	0.12338
	RF	0.46120	0.52012	0.08466	0.16598
	BRT	0.5644	0.56014	0.01672	0.05316

Table S2 Variable importance per iteration of control locations, 2011/12. Mean importance of environmental variables (Sea Surface Temperature, SST; Chlorophyll-a, chl-a; thermal front frequency, Tfreq; depth) over model runs (10-fold cross-validation) per iteration of control locations, for each model algorithm (Generalised Additive Models, GAM; Maximum Entropy modelling, MaxEnt; Random Forest, RF; Boosted Regression Trees, BRT). Mean of Relative Importance to the model Coefficients (RICC) metric over successive iteration of control locations.

Control Location Iteration	Model Algorithm	Variable Importance (mean over 10 runs per pseudo-absence iteration)			
		SST	Chl- <i>a</i>	TFreq	Depth
1	GAM	0.9427	0.0941	0.0669	0.1390
	MaxEnt	0.5170	0.2031	0.4323	0.1567
	RF	0.4893	0.2765	0.2358	0.1887
	BRT	0.5819	0.2770	0.2378	0.0778
2	GAM	0.9277	0.0861	0.0580	0.1997
	MaxEnt	0.5942	0.2101	0.2982	0.1814
	RF	0.5094	0.2904	0.2906	0.1838
	BRT	0.5621	0.3188	0.2943	0.0681
3	GAM	0.9310	0.1234	0.0423	0.1522
	MaxEnt	0.4932	0.1673	0.1621	0.2250
	RF	0.5145	0.2910	0.2369	0.1892
	BRT	0.6279	0.3018	0.1764	0.0690
4	GAM	0.8950	0.0873	0.1362	0.1821
	MaxEnt	0.7395	0.3093	0.5689	0.1517
	RF	0.5737	0.2619	0.2485	0.2424
	BRT	0.6172	0.2780	0.2186	0.1113
5	GAM	0.9123	0.1021	0.0842	0.1557
	MaxEnt	0.4390	0.1841	0.1300	0.2316
	RF	0.5027	0.2708	0.2339	0.2138
	BRT	0.5784	0.3132	0.2165	0.0763
mean of means	GAM	0.92174	0.09860	0.07752	0.16574
	MaxEnt	0.55658	0.21478	0.31830	0.18928
	RF	0.51792	0.27812	0.24914	0.20358
	BRT	0.59350	0.29776	0.22872	0.0805

Table S3 Model performance metrics per iteration of control locations, 2009/10.

Evaluation metrics (Area Under Receiver Operating Curve, AUC; True Skill Statistic, TSS). Mean over model runs (10-fold cross-validation) per iteration of control locations, for each model algorithm (Generalised Additive Models, GAM; Maximum Entropy modelling, MaxEnt; Random Forest, RF; Boosted Regression Trees, BRT).

Control Location Iteration	Evaluation Metric	Model Algorithm (mean over 10 runs per Pseudo-Absence iteration)			
		GAM	MaxEnt	RF	BRT
1	AUC	0.9362	0.9166	0.9511	0.9407
	TSS	0.8172	0.7599	0.8273	0.8094
	Boyce Index	0.9155	0.9391	0.8635	0.681
2	AUC	0.9520	0.9358	0.9641	0.9552
	TSS	0.8383	0.7967	0.8632	0.8452
	Boyce Index	0.9174	0.9343	0.8215	0.6572
3	AUC	0.9593	0.9287	0.9431	0.9374
	TSS	0.8209	0.7871	0.8164	0.8110
	Boyce Index	0.9154	0.9695	0.8195	0.6966
4	AUC	0.9494	0.9315	0.9604	0.9518
	TSS	0.8466	0.7749	0.8352	0.8256
	Boyce Index	0.9164	0.9624	0.8336	0.7599
5	AUC	0.9337	0.9253	0.9428	0.9369
	TSS	0.7956	0.7514	0.7963	0.7967
	Boyce Index	0.9419	0.8436	0.8263	0.7701
Mean of means	AUC	0.9421	0.9276	0.9523	0.9444
	TSS	0.8237	0.7740	0.8277	0.8176
	Boyce Index	0.9213	0.9300	0.8329	0.7130

Table S4 Model performance metrics per iteration of control locations, 2011/12.

Evaluation metrics (Area Under Receiver Operating Curve, AUC; True Skill Statistic, TSS). Mean over model runs (10-fold cross-validation) per iteration of control locations, for each model algorithm (Generalised Additive Models, GAM; Maximum Entropy modelling, MaxEnt; Random Forest, RF; Boosted Regression Trees, BRT).

Control Location Iteration	Evaluation Metric	Model Algorithm (mean over 10 runs per Pseudo-Absence iteration)			
		GAM	MaxEnt	RF	BRT
1	AUC	0.9311	0.9058	0.9461	0.9334
	TSS	0.7824	0.7214	0.8111	0.7745
	Boyce Index	0.9125	0.9484	0.9040	0.8692
2	AUC	0.9344	0.9055	0.9551	0.9418
	TSS	0.7748	0.7019	0.8196	0.7810
	Boyce Index	0.8638	0.8955	0.9065	0.8397
3	AUC	0.9463	0.9126	0.9658	0.9496
	TSS	0.7892	0.7136	0.8345	0.7842
	Boyce Index	0.8778	0.8398	0.8697	0.8447
4	AUC	0.9365	0.9122	0.9581	0.9403
	TSS	0.7871	0.7399	0.8394	0.7908
	Boyce Index	0.8968	0.9237	0.8989	0.8564
5	AUC	0.9376	0.9143	0.9565	0.9437
	TSS	0.7842	0.7154	0.8369	0.7908
	Boyce Index	0.9206	0.9181	0.9197	0.8976
Mean of means	AUC	0.9372	0.9101	0.9563	0.9418
	TSS	0.7835	0.7184	0.8283	0.7843
	Boyce Index	0.8943	0.9051	0.8998	0.8615

Table S5 Model Parameterisation settings

GAM	package = 'mgcv', family = 'binomial' (link = 'logit'), type = 's' (spline-based smooth), model formula =
RF	number of trees = 500, node size = 5; Boosted Regression Trees
BRT	distribution = 'bernoulli', number of trees = 2500, shrinkage = 0.001, bag fraction = 0.5, train fraction = 1, cross-validation folds = 3
MaxEnt	maximum training iterations = 200, linear/quadratic/product/threshold/hinge features enabled, default prevalence = 0.5